

**A peer-reviewed version of this preprint was published in PeerJ on 2 November 2018.**

[View the peer-reviewed version](https://peerj.com/articles/5830) (peerj.com/articles/5830), which is the preferred citable publication unless you specifically need to cite this preprint.

Cicala F, Cisterna-Céliz JA, Moore JD, Rocha-Olivares A. 2018. Structure, dynamics and predicted functional role of the gut microbiota of the blue (*Haliotis fulgens*) and yellow (*H. corrugata*) abalone from Baja California Sur, Mexico. PeerJ 6:e5830 <https://doi.org/10.7717/peerj.5830>

# Structure, dynamics and predicted functional ecology of the gut microbiota of the blue (*Haliotis fulgens*) and yellow (*H. corrugata*) abalone from Baja California Sur, Mexico

Francesco Cicala<sup>1</sup>, José Alejandro Cisterna-Céliz<sup>1</sup>, James Douglas Moore<sup>2</sup>, Axayácatl Rocha-Olivares<sup>Corresp. 1</sup>

<sup>1</sup> Biological Oceanography, Centro de Investigación Científica y de Educación Superior de Ensenada, Ensenada, B.C. Mexico, Mexico

<sup>2</sup> Bodega Marine Laboratory, University of California, Davis, Bodega Bay, California, United States

Corresponding Author: Axayácatl Rocha-Olivares  
Email address: arocha@cicese.mx

The gastro-intestinal (GI) microbiota of abalone contains a highly complex bacterial assemblage playing an essential role in the overall health of these gastropods. The gut bacterial communities characterized so far reveal considerable interspecific variability, likely resulting from bacterial interactions and constrained by the ecology of their host species; however, they remain poorly investigated. Additionally, the extent to which structural changes in the microbiota entail functional shifts in metabolic pathways of bacterial communities remains unexplored. In order to address these questions, we characterized the gut microbiota of the northeast Pacific blue (*Haliotis fulgens* or HF) and yellow (*Haliotis corrugata* or HC) abalone by 16S rRNA 454 pyrosequencing to shed light on: (i) their gut microbiota structure; (ii) how bacteria may interact among them; and (iii) predicted shifts in bacterial metabolic functions associated with the observed structural changes. Our findings revealed that *Mycoplasma* dominated the GI microbiome in both species. However, the structure of the bacterial communities differed significantly in spite of considerable intra-specific variation. This resulted from differences of the species with most reads in each GI metagenome, suggesting host-specific adaptation of bacterial lineages to these sympatric abalone. We hypothesize that the presence of exclusive OTUs in each microbiota may relate to host-specific differences in competitive pressure. Significant differences in bacterial diversity were found for the explored metabolic pathways between species despite their functional overlap. A more diverse array of bacteria contributed to each function in HC, whereas a single or much fewer OTUs were generally observed in HF. The structural and functional analyses allowed us to describe a deep taxonomic and functional split between the microbiota of HF and HC abalone.

1 **Structure, dynamics and predicted functional ecology of the gut microbiota of**  
2 **the blue (*Haliotis fulgens*) and yellow (*H. corrugata*) abalone from Baja**  
3 **California Sur, Mexico.**

4

5

6 Francesco Cicala<sup>1</sup>, José Alejandro Cisterna Céliz<sup>1</sup>, James D. Moore<sup>2</sup>, Axayácatl Rocha-Olivares<sup>1</sup>

7

8 <sup>1</sup> Molecular Ecology Laboratory, Department of Biological Oceanography, CICESE, Carretera  
9 Tijuana-Ensenada km 107, Ensenada Baja California, 22860 México.

10

11 <sup>2</sup> Bodega Marine Laboratory, University of California at Davis, P. O. Box 247, Bodega Bay, CA,  
12 USA

13

14

15 Corresponding Author:

16 Axayácatl Rocha-Olivares<sup>1</sup>

17 Carretera Tijuana-Ensenada km 107, Ensenada, Baja California, 22860, México.

18 Emai address: [arocha@cicese.mx](mailto:arocha@cicese.mx)

19

20

21 **ABSTRACT**

22

23 The GI microbiota of abalone contains a highly complex bacterial assemblage playing an  
24 essential role in the overall health of these gastropods. The gut bacterial communities characterized  
25 so far reveal considerable interspecific variability, likely resulting from bacterial interactions and  
26 constrained by the ecology of their abalone host species; however, they remain poorly investigated.  
27 Additionally, the extent to which structural changes in the microbiota entail functional shifts in  
28 metabolic pathways of bacterial communities remains unexplored. In order to address these  
29 questions, we characterized the gut microbiota of the northeast Pacific blue (*Haliotis fulgens* or  
30 HF) and yellow (*Haliotis corrugata* or HC) abalone by *16S rRNA* 454 pyrosequencing to shed  
31 light on: (i) their gut microbiota structure; (ii) how bacteria may interact among them; and (iii)  
32 predicted shifts in bacterial metabolic functions associated with the observed structural changes.  
33 Our findings revealed that *Mycoplasma* dominated the GI microbiome in both species. However,  
34 the structure of the bacterial communities differed significantly in spite of considerable intra-  
35 specific variation. This resulted from changes in predominant species composition in each GI  
36 metagenome, suggesting host-specific adaptation of bacterial lineages to these sympatric abalone.  
37 We hypothesize that the presence of exclusive OTUs in each microbiota may relate to host-specific  
38 differences in competitive pressure. Significant differences in bacterial diversity were found for  
39 the explored metabolic pathways between species despite their functional overlap. A more diverse  
40 array of bacteria contributed to each function in HC, whereas a single or much fewer OTUs were  
41 generally observed in HF. The structural and functional analyses allowed us to describe a deep  
42 taxonomic and functional split between the microbiota of HF and HC abalone.

43

## 44 Background

45

46 The gastro-intestinal (GI) tract of metazoans may be considered a highly complex  
47 ecosystem inhabited by a large number of bacteria [1]. For instance, the commensal microbiota  
48 harbored by the human GI tract far exceeds the total number of cells in the entire human body, and  
49 their collective genome (microbiome) is orders of magnitude larger than our own [1,2]. Moreover,  
50 the GI microbiome has been associated with essential physiological activities such as food  
51 digestion, nutrient assimilation, and defense against invasion of foreign bacterial species; which  
52 in turn may prevent epidemiologic outbreaks [3–5]. Also, functional studies have revealed that the  
53 relationship between the gut microbiome and its host may be so close that bacteria may be directly  
54 involved in the maturation of the GI tract of the hosts species [2,6,7].

55 As documented by cultured and uncultured approaches, the composition of the abalone gut  
56 microflora may be influenced by a great variety of factors such as diet, environmental conditions  
57 and ontogenetic stages [3,4,8–11]. Also, the use of probiotics has revealed that interspecific  
58 bacterial relationships may also shape the final gut microbiome composition of several marine  
59 invertebrates, including abalone [12–14]. Overall, these factors may explain the consistent  
60 differences in the gut microbiome of abalone species studied so far. In this context, the most  
61 abundant bacteria in homogenate samples of the entire GI of *H. discus hannai* were fermenter  $\gamma$ -  
62 *proteobacteria*, such as *Vibrio haliotocoli* as well as other *Vibrio* species,  $\alpha$ - *proteobacteria*,  
63 *Mollicutes* and *Fusobacteria* [10,16]. Moreover, the intestinal microflora (from stomach to anus)  
64 of *Haliotis diversicolor* was dominated by *Mollicutes*, *Flammeovirga*, as well as  $\beta$  and  $\alpha$ -,  $\gamma$ - and  
65  $\delta$ - *proteobacteria* [17]. In contrast, the bacterial composition of *H. gigantea* (from homogenate  
66 samples of the entire GI) appears less complex with a preponderance of  $\gamma$ - *proteobacteria* and  
67 *Mollicutes* [14].

68 The peninsula of Baja California harbors seven exploitable abalone species [18], two of  
69 which, the blue abalone *Haliotis fulgens* (HF, henceforth) and the yellow abalone *Haliotis*  
70 *corrugata* (HC, henceforth), sustain a high-valued fishery in the NW Mexican Pacific [18,19].  
71 Despite the importance of the GI microbiomes for the survival of these abalone species, no efforts  
72 have been made to characterize them. Furthermore, it is equally uncertain which factors may shape  
73 their final composition as well as the functional roles played by the most representative bacterial  
74 groups.

75            Here, with the aim of addressing these questions, we analyze the structure of the GI  
76 microbiota of wild- caught specimens of HC and HF by means of *16S rRNA* amplification and 454  
77 pyrosequencing (Roche). Additionally, we analyze the functional shifts involved in structural  
78 changes using a predictive metagenomic analysis to focus on 86 genes involved in several  
79 metabolic pathways.

80

## 81 **Materials and Methods**

82

83 Sample collection and genetic analyses.

84

85 Wild abalone (n = 31 HF, n = 35 HC) were sampled from the commercial harvested along  
86 the Pacific coast of central Baja California, Mexico. Approximately 30 mg of post esophageal  
87 tissue were dissected from visually healthy animals bearing no signs of the withering syndrome  
88 [24], and immediately transferred to sterile 1.5 ml microcentrifuge tubes containing molecular  
89 grade ethanol, until further analysis. Abalone and bacterial DNA was extracted and purified from  
90 preserved tissues using DNeasy blood & tissue kit (Qiagen, Valencia, CA, USA) following  
91 manufacturer's protocols.

92 A fragment of the bacterial ribosomal *16S rRNA* spanning V1-V3 regions was PCR  
93 amplified using universal eubacterial primers 28F: 5' - GAGTTTGATCNTGGCTCAG - 3' [45]  
94 and 519R: 5' - GTNTTACNGCGGCKGCTG - 3' [46]. PCR reactions (20 µl) contained: 1X PCR  
95 Buffer (Kapa Biosystems, Woburn, MA, USA), 1.5 mM magnesium chloride (Kapa Biosystems,  
96 Woburn, MA, USA), 0.2 mM dNTPs (New England Biolabs), 0.5 µM each primer, 0.4 mM bovine  
97 serum albumin (New England Biolabs, Beverly, MA, USA), 1U *Taq* polymerase (Kapa  
98 Biosystems, Woburn, MA, USA), and 100 ng purified DNA. Thermal cycling consisted of an  
99 initial incubation at 94 °C for 4 min, followed by 40 cycles of: 94 °C for 1 min; 62°C for 30 sec.  
100 and 72 °C for 30 sec., and a final incubation of 8 min at 72 °C. Confirmation of amplification was  
101 carried out by 1.5% agarose gel electrophoresis. Amplicons were subsequently tagged using Roche  
102 454 adaptors and multiplex identifier (MID) tags for each organism, following the bacterial tag-  
103 encoded FLX amplicon pyrosequencing (bTEFAP) approach of Dowd *et al.* [47]. Following  
104 normalization, Roche 454 pyrosequencing was carried out in a GS FLX Titanium platform by  
105 Research and Testing Laboratory (Lubbock, TX).

106

107 Bioinformatic analyses

108

109 The *16S rRNA* reads were analyzed using Quantitative Insights Into Microbial Ecology  
110 (QIIME) software version 1.9.1 [48]. The first step consisted in demultiplexing and primer  
111 removal. Subsequently, reads were filtered according to Phred quality scores obtained from the

112 454 pyrosequencing. Acceptance quality criteria consisted of: (i) minimum and maximum lengths  
113 of 250 and 550 bp, respectively; (ii) default minimum quality Phred score of 25; (iii) no mismatch  
114 in primer sequences and MID-tag; (iv) maximum homopolymer length of 8 bp.

115 Sequences that met quality criteria were clustered in operational taxonomic units (OTUs)  
116 at 97% sequence similarity using the UCLUST algorithm [49]. The longest sequence from each  
117 OTU was selected as representative and these were subsequently aligned using Python Nearest  
118 Alignment Space Termination (also PyNASt) algorithm [50]. ChimeraSlayer [51] was used to  
119 detect and remove chimeras/singleton reads as implemented in QIIME. An additional chimera  
120 control test and taxonomic assignment were carried out by a BLAST search against the SILVA  
121 database (<http://www.arb-silva.de/>).

122

## 123 Ecological analysis

124

125 The number of reads of each OTU was used as an abundance proxy to estimate  
126 metagenomic diversity and structure of the abalone gut microbiota. Species richness (S), Shannon-  
127 Wiener (H) and Equitability (J) indices were calculated using Past V. 2.17c [52]. Taxonomic  
128 differences between abalone species, were evaluate by both Student t-tests using R [53] and by a  
129 linear discriminant analysis (LDA) effect size (LEfSe) [54]. To assess how exhaustively bacterial  
130 communities of both abalone species were sampled, rarefaction curves of discovered OTUs were  
131 generated for increasing numbers of sampled abalone. Also, OTU abundance was used to compute  
132 the non-parametric species richness estimator Chao 1 [55]. Rarefaction curves were obtained using  
133 the EstimateS V.9.0.1 program [56]. Microbiome community structure was evaluated using non-  
134 paramteric multidimensional scaling (MDS) analyses using Bray-Curtis and Sorensen similarity  
135 indices based on read abundance and on presence/absence, respectively, as implemented in  
136 PRIMER V.6 [57]. The statistical comparison of MDS results was performed with ANOSIM as  
137 implemented in Past V. 2.17c [52]. To determine which OTUs were primarily responsible for the  
138 similarities within each species and dissimilarity between HF and HC, a SIMPER analysis with  
139 square root transformed data was performed using PRIMER V.6 [57].

140 Bacterial interactions in the microbiomes of both abalone species were estimated using  
141 Jaccard distance ( $J_d$ ) as implemented in PRIMER V.6 [57].  $J_d$  is a measure of dissimilarity for all  
142 pairwise combinations of a data set [25] and was calculated using OTUs presence/absence.  $J_d$



143 values close to 0 (from 0 to 0.33) were interpreted as co-occurrence (or putative mutualistic  
144 relationships) and values close to 1 (from 0.68 to 1) as interactions leading to exclusion (or putative  
145 competitive) [59]; whereas intermediate values were considered neutral relationships. We  
146 followed two approaches in the estimation of bacterial interactions. First, we computed  $J_d$  distances  
147 between all pairs of OTUs obtained from individual reads (putative species level). However, these  
148 mathematical results may not necessarily reflect a biological interaction. In order to improve the  
149 analysis, we posited that phylogenetically-related species share ecological functional attributes  
150 [23]. Thus, in an attempt to cluster bacterial species with similar functions and explore ecological  
151 interactions within those groups, we grouped OTUs at the  $\geq 90\%$  DNA sequence similarity and  
152 recomputed mean Jaccard distances within those groups only (i.e., referred to as “phylogenetic  
153 groups” henceforth). Distance matrices were computed with Geneious R9 [60]. Finally, in order  
154 to test the hypothesis that abundant bacteria in the microbiomes are subject to less competition and  
155 more neutral or positive interactions, we correlated the mean Jaccard distance (or  $\bar{J}_d$ ) of each OTU  
156 with its abundance (i.e., number of reads).

157

158

159 Functional prediction of metagenomes

160

161 A phylogenetic investigation of communities by reconstruction of unobserved states  
162 (PICRUSt) [61] was carried out to predict the functional attributes of metabolic genes from HF  
163 and HC GI microbiomes. Briefly, PICRUSt is a bioinformatic approach that uses information from  
164 a number of genetic markers, including the *16S rRNA*, to predict the metagenome functional  
165 content [61,62]. These predictions were obtained by matching our *16S rRNA* gene sequences  
166 against the prearranged genomic KEGG database [61,62]. The central result of PICRUSt consists  
167 of a table reporting the functional gene frequencies known as KEGG Orthologs (or KOs). KOs are  
168 hierarchically organized in sets of homologous sequences with known molecular function and  
169 assigned to biological pathways. We analyzed the data using the raw KOs counts as well as  
170 categorizing them by biological pathway. PICRUSt analyses use Greengenes  
171 (<http://greengenes.lbl.gov/cgi-bin/nph-index.cgi>) as taxonomic and functional reference database.  
172 To implement quality control, we computed weighted nearest sequenced taxon index (NSTI)  
173 values for each individual metagenome. NSTI was developed to evaluate the prediction accuracy

174 of PICRUSt, since it reflects the average genetic distance (measured as number of substitutions  
175 per site) between an OTU against a reference genome [61,62]. Following suggested guidelines  
176 [61], we eliminated observations with a NSTI higher than 0.17.

177 In order to assess the contribution of individual OTUs to predicted KO functions, first we  
178 focused our analyses on genes involved in metabolic pathways (KEGG IDs from EC:1.1.1 to  
179 EC:6.5.1). Next, we categorized the relative importance of KO genes by ranking them according  
180 to their raw counts. These counts were obtained with PICRUSt v.1.1.0 [61] and were log  
181 normalized [63]. Finally, we focused our attention on a random subset (n =10) of KOs with the  
182 highest counts, as a first order analyses to characterize functional differences between these  
183 microbiomes. These analyses were carried out with the script *metagenome contributions.py*.

184 Finally, in order to compare the predicted ecological functions and the KOs abundance  
185 between microbiomes of both species of abalone, non-parametric MDS analysis based on Bray-  
186 Curtis similarity using  $\log(x+1)$  transformation of data were performed in PRIMER V6 [57].

## 187 Results

188

### 189 Pyrosequencing and metagenome structure

190

191 Pyrosequencing yielded 451,095 raw *16S rRNA* reads of which 245,779 (54.5%) met  
192 quality criteria and were assigned to 281 OTUs, of which 87 had no match to databases (i.e., “No  
193 Hit”). The most abundant phyla (number of OTUs in parenthesis), included *Bacteroidetes* (13),  
194 *Fusobacteria* (14), *Proteobacteria* (56) and *Tenericutes* (96). Additionally, classified OTUs were  
195 assigned to 25 families and 47 genera (Table S1). The five most abundant OTUs ( $n > 15876$  reads)  
196 were assigned to class *Mollicutes* (order *Mycoplasmatales*). Notably, LEfSe analysis revealed that  
197 63 of 96 *Mollicutes* OTUs were exclusive to either in HC or HF (Fig. S1). Similar results were  
198 observed for other predominant bacterial families such as *Fusobacteriaceae* and *Vibrionaceae*  
199 (Fig. S1).

200 The classes *Fusobacteria*, *Mollicutes*,  $\alpha$ - and  $\gamma$ -*protobacteira* comprised 99% of the  
201 identifiable reads. Rarefaction curves suggest that the bacterial communities were sufficiently  
202 sampled in both abalone species, given their asymptotic shape and the proximity of the observed  
203 number of taxa in each species to CHAO 1 estimates (Fig. 1). Species richness was significantly  
204 higher ( $t = 6.07$ ;  $p < 0.01$ ) in HF (mean  $\pm$  S.D. HF:  $56.45 \pm 12.49$ ; HC:  $36.66 \pm 13.16$ ).

205 Despite their similar composition at the class level (Fig. 2), MDS analyses at the highest  
206 taxonomic resolution revealed a clear-cut structural difference between the metagenomes of both  
207 species, in the presence of considerable intraspecific variation, using read numbers as proxy for  
208 abundance (Fig. 3) or solely on the basis of presence/absence data (Fig. S2). Significant  
209 interspecific differentiation was corroborated by ANOSIM analyses in both cases ( $R_{\text{abundance}} =$   
210  $0.72$ ;  $p < 0.001$ ;  $R_{\text{presence/absence}} = 0.73$ ;  $p < 0.001$ ).

211 Jaccard distances revealed that interspecific relationships among OTUs changed by an  
212 order magnitude with most involving competition (HC: 24,242 and HF: 24,118), followed by  
213 neutral (HC: 1321 and HF: 2123) and a smaller number of mutualistic interactions (HC: 315 and  
214 HF: 323). Furthermore, the  $\bar{J}_d$  of the majority of OTUs decreased significantly with increasing read  
215 number in both species ( $p < 0.001$ ; Fig. 4). The same trend was observed within phylogenetic  
216 groups (Fig. S3).

217

## 218 Functional profiling

219

220 Most abalone possessed mean NSTI values from 0.07 to 0.17, except for seven HCs with higher  
221 values that made them unreliable; hence they were excluded from further analyses. PICRUSt  
222 identified 4,201 KOs genes (Table S2) involved in 262 metabolic functions (Table S3). A one  
223 order of magnitude drop in log-normalized abundance was observed in the ranking of KOs (Fig  
224 S4); hence, *metagenome contributions* analysis was carried out on a random set of 10 of the 86  
225 most abundant Kos (i.e. Log (KOs counts > 4). According to PICRUSt, the metabolic functions in  
226 the HF microbiomes were generally enriched by one primary OTU, whereas many more OTUs  
227 contributed to the same function in HC (Fig.5). MDS analyses performed using both KOs genes  
228 and ecological function counts revealed no clear functional separation of the GI microbiota of both  
229 species, even though the scatter of individual microbiomes is much larger in HC, which is  
230 consistent with its higher diversity (Fig. 6).

## 231 Discussion

232

233 Abalone microbiome composition and dynamics

234

235 Our data revealed that the post esophageal microflora of HC and HF are dominated by the  
236 same bacterial classes. *Mollicutes*, mostly represented by *Mycoplasma* spp., was by far the most  
237 abundant class, followed by *Fusobacteria*,  $\alpha$ -*proteobacteria* and  $\gamma$ -*proteobacteria*, with the latter  
238 represented by the genera *Vibrio* and *Francisella*. These bacteria have also been found dominating  
239 in the GI microbiota of other abalone species (*H. discus hannai*, *H. diversicolor* and *H. gigantean*  
240 [10,14,16,17]). Even though the taxonomic composition of HC and HF GI microbiotas bears  
241 resemblance at high taxonomic levels, the species level composition showed significant  
242 differences. For instance, several *Mycoplasma* species predominant in one abalone were either  
243 absent or at low abundance in the other. Furthermore, all *Vibrio* spp. presented a higher prevalence  
244 in HC (Fig. S1). Notably, *Vibrio halioticoli* was absent in both HF and HC whereas it has been  
245 found at prevalence ranging from 40 to 65% in the GI of other marine invertebrates, including  
246 several abalone species [9]. The discrepancy may in part be related to the anatomical source of the  
247 microbiomes, our samples come from post esophageal tissue only whereas other studies have  
248 analyzed the entire GI tracts [14,16]. Consequently, the presence of *V. halioticoli* in the rest of GI  
249 tissues of HC and HF should be explored.

250 Our findings suggest that for most bacterial species their abundance decreased with increasing  
251 competition (lower  $\bar{J}_d$  values), as observed for *Mycoplasma*. Furthermore,  $\bar{J}_d$  for a single bacterium  
252 changed according to its host, which suggests that the same bacterial species faces different  
253 competitive pressures depending on the microbiota composition (Table S4). In other words,  
254 bacteria that may avoid competition in one microbiome, may be out competed in the other.  
255 However, this interpretation assumes untested hypothetical interspecific interactions [22].  
256 Consequently, the same analysis was conducted focusing on genetically similar ( $\geq 90\%$  similarity)  
257 OTUs, assuming that genetically related bacteria may share similar ecological roles [23]. This  
258 second approach produced similar results (Fig.S1), which may support the analysis carried out  
259 using all pairs of OTUs.

260 Some pathogenic bacteria, such as *Candidatus Xenohalotis californiensis* and *Francisella*,  
261 were observed in the microbiomes of healthy abalone. The former has been recognized as the

262 etiological agent of the withering syndrome, a chronic wasting disease that possibly affects all  
263 north American abalone species [24]. This bacterium is a pleomorphic, gram-negative  
264 coccobacillus that inhabits abalone gastrointestinal epithelia and is considered an obligate  
265 endoparasite, like other *Rickettsiales* [25–27]. We observed the presence of *Candidatus*  
266 *Xenohaliotis californiensis* in healthy blue and yellow abalone, which supports that the presence  
267 of this pathogen is not sufficient to trigger withering syndrome as previously proposed [28].  
268 Moreover, its absence and/or low intensity in abalone with morphological and histological signs  
269 of withering syndrome has already been reported [28–30]. Accordingly, we posit that further  
270 investigations are needed to reveal all the factors involved in withering syndrome outbreaks.

271 *Francisella* is a  $\gamma$ - proteobacterium and has previously been found in abalone microbiota  
272 [31]. It is a non-motile, pleomorphic gram-negative coccobacillus mainly known to be a facultative  
273 intracellular parasite of a wide range of hosts, including humans [31,32]. At the moment, this genus  
274 consists of five validated species [31]. Additionally, a novel species named *F. halioticida* [31] has  
275 been isolated from a die-off of farmed *H. gigantea* in Japan, for which it was identified as the  
276 etiological agent [33]. The *Francisella* ribotype detected in *H. corrugata* from Mexico was only  
277 89% similar to *F. halioticida* 16S rRNA sequence (Genbank accession number NR\_118116),  
278 which suggests a different species. Moreover, the presence of this bacterium in only HC organisms  
279 and its low prevalence (n = 2), suggests that this strain should not be considered an established  
280 member of the HC abalone bacterial core. Also, our limited data do not support the pathogenicity  
281 of the detected strain.

282 Finally, many bacterial genera were detected in low read frequencies and prevalences. Some  
283 of these (e.gr., *Acinetobacter*, *Alteromonas*, *Bacillus*, *Flavobacterium*) bear strong relationships  
284 with macroalgae [34] and may have been ingested while grazing.

285

286

287 Ecological functions of the abalone microbiome

288

289 According to the MDS of KOs gene counts and ecological functions, the inferred functionality  
290 of the GI microbiota of HF appears less variable than that of HC, which may reflect a higher degree  
291 of diet specialization. The diet diversity of wild HF in Baja California has been shown to be more  
292 limited and dominated by *Phyllospadix torreyi* (47%) and algae in the order *Gelidiales* (13%). On

293 the other hand, the diet of sympatric wild HC is more diverse consisting of different species of  
294 Phaeophyceae (10-20%), Rhodophyta (20%) and *Gelidiales* (20%) among others [35]. Possibly,  
295 those dietary preferences may be the result of bathymetric adaptations; indeed, HC are generally  
296 found in relative deep waters (between 10-20m), whereas HF generally inhabit shallow regions  
297 (between 3-10m) [35].

298 In the microbiota of both HC and HF, *Mycoplasma* contributed to all predicted KEGG.  
299 However, a given KO was generally enriched by a single predominant *Mycoplasma* OTU in HF,  
300 whereas in HC it was generally enriched by two or more *Mycoplasma* as well as other bacterial-  
301 OTUs (Fig.5). In other words, our results not only support that different *Mycoplasma* species may  
302 be highly host-specific [36], but also that they may also be highly specific to ecological tasks  
303 and/or to specific steps along a metabolic route. This may also be reflected by the relative low  $J_d$   
304 (interpreted as absence of competitive interactions) of *Mycoplasma* OTUs. Indeed, ecological  
305 specialization should translate into niche partitioning and a reduction of inter-specific competition  
306 (Table S4).

307 To our knowledge, this is the first time that the ecological functions of *Mycoplasma* have  
308 been explored by a predictive analysis. *Mycoplasma* possess the smallest genome size among  
309 bacteria [7]; because of their small genome and number of genes, *Mycoplasma* species have been  
310 considered as obligate parasites and/or commensals [7,37]. Furthermore, our results suggest that  
311 these bacteria should be considered members of the bacterial core in the GI microflora of abalone.

312 *Vibrio* was the second most common genus observed enriching the majority of predicted  
313 KEGG. These bacteria are Gram-negative  $\gamma$ -*proteobacteria* that include both pathogenic and non-  
314 pathogenic species [38–40]. As it is the case in Asian abalone [9,14,17], our results confirm that  
315 *Vibrio* may be considered one of the main components of abalone GI microbiota in the eastern  
316 Pacific, at least in HC. Also, *Vibrio* has been found to play a pivotal role converting alginate to  
317 acetic acid [9,10]. In *Vibrio cholera*, possibly the best studied *Vibrio* species, the genome has been  
318 found to be dynamic, continuously acquiring and losing genes over time [38,41]. Consequently,  
319 as suggested by the PICRUST analysis, *Vibrio* may be involved in a large number of ecological  
320 functions in the GI of abalone. We also speculate that the dominance of *Vibrio* in HC may  
321 contribute to their ability to process a wider spectrum of food sources.

322 PICRUST analysis also revealed that several other bacteria may play major roles in several  
323 metabolic and/or enzyme production pathways. *Fusobacteriaceae* (mainly represented by

324 *Psychrilyobacter*) are obligate anaerobic gram-negative bacilli and are generally found in anoxic  
325 marine sediments. Species in this bacterial family have been detected in several marine  
326 invertebrate hosts such as shrimp [42], muricid snail [43], and abalone [16] and have been shown  
327 to be involved in the degradation of organic compounds [16,42,44]. Our findings suggest that these  
328 bacteria may be involved in several metabolic and/or enzyme production pathways such as  
329 glycerophospholipid metabolism (K00057), starch and sucrose metabolism (K07024) and seleno-  
330 compound metabolism (K117170), among others, where they may take part in the production of  
331 dehydrogenases, lyases and other hydrolytic enzymes.

332



333 **Conclusion**

334

335 Using bTEFAP we characterized the microbiota of two commercially important and sympatric  
336 abalone in Mexico. Our results revealed novel microbiomes with significant shifts in bacterial  
337 species composition between them and with other species of abalone in the world. Given that these  
338 structural differences in microbiome composition do not necessarily result in distinct functional  
339 signatures, we posit that interspecific bacterial competition and the ecological differences of their  
340 host (i.e., diet and bathymetric distribution) may be responsible for these differences. These results  
341 may provide baseline references for future temporal and spatial sampling, and to assess  
342 microbiome changes related to ontogeny as well as physiological/health conditions. Additional  
343 efforts should also be directed towards understanding the roles of environment variables or other  
344 factors that may alter the GI microbiome of abalone.

345

346 **Acknowledgements**

347

348 We are grateful to Ms. Ashley Vater and Andrea Lievana-MacTavish for a critical assessment of  
349 an earlier version of the manuscript.

350

## 351 REFERENCES

352

353 1. Backhed F. Host-Bacterial Mutualism in the Human Intestine. *Science* 2005;307:1915–20.  
354 doi:10.1126/science.1104816

355

356 2. Bates JM, Mittge E, Kuhlman J, Baden KN, Cheesman SE, Guillemin K. Distinct signals from  
357 the microbiota promote different aspects of zebrafish gut differentiation. *Dev. Biol.*  
358 2006;297:374–86. doi: 10.1016/j.ydbio.2006.05.006

359

360 3. ten Doeschate KI, Coyne VE. Improved growth rate in farmed *Haliotis midae* through  
361 probiotic treatment. *Aquaculture*; 2008;284:174–9. doi: 10.1016/j.aquaculture.2008.07.018

362

363 4. Zhao J, Shi B, Jiang QR, Ke CH. Changes in gut-associated flora and bacterial digestive  
364 enzymes during the development stages of abalone (*Haliotis diversicolor*). *Aquaculture*.  
365 2012;338–341:147–53. doi: 10.1016/j.aquaculture.2012.01.016

366

367 5. Blaut M, Clavel T. Metabolic diversity of the intestinal microbiota: implications for health and  
368 disease. *J. Nutr.* 2007;137:751S–5S.

369

370 6. Bry L, Falk PG, Midtvedt T, Gordon JI. A model of host-microbial interactions in an open  
371 mammalian ecosystem. *Science*. 1996. p. 1380–3.

372

373 7. Bano N, DeRae Smith A, Bennett W, Vasquez L, Hollibaugh JT. Dominance of *Mycoplasma*  
374 in the guts of the Long-Jawed Mudsucker, *Gillichthys mirabilis*, from five California salt  
375 marshes. *Environ. Microbiol.* 2007;9:2636–41. doi:10.1111/j.1462-2920.2007.01381.x

376

377 8. Meryandini A, Junior MZ, Rusmana I. The Role of Agarolytic Bacteria in Enhancing  
378 Physiological Function for Digestive System of Abalone (*Haliotis asinina*). *J. Appl.*  
379 *Environ.Biol. Sci.* 2015;5:49–56.

380

381 9. Sawabe T, Setoguchi N, Inoue S, Tanaka R, Ootsubo M, Yoshimizu M, et al. Acetic acid  
382 production of *Vibrio halioticoli* from alginate: A possible role for establishment of abalone *V.*  
383 *halioticoli* association. *Aquaculture*. 2003;219:671–9. doi: 10.1016/S0044-8486(02)00618-X

384

385 10. Tanaka R, Sugimura I, Sawabe T, Yoshimizu M, Ezura Y. Gut microflora of abalone  
386 *Haliotis discus hannai* in. *Fish. Sci.* 2003;69:951–8. doi: 10.1046/j.1444-2906.2003.00712

387

388 11. Pang SJ, Xiao T, Bao Y. Dynamic changes of total bacteria and *Vibrio* in an integrated  
389 seaweed–abalone culture system. *Aquaculture*. 2006;252:289–97. doi:

390 10.1016/j.aquaculture.2005.06.050

391

392 12. Macery B., Coyne VE. Improved growth rate and disease resistance in farmed *Haliotis midae*  
393 through probiotic treatment. *Aquaculture*. 2004;245:249–61. doi:

394 10.1016/j.aquaculture.2004.11.031

395

396

- 397 13. Rungrassamee W, Klanchui A, Maibunkaew S, Chaiyapechara S, Jiravanichpaisal P,  
398 Karoonuthaisiri N. Characterization of intestinal bacteria in wild and domesticated adult black  
399 tiger shrimp (*Penaeus monodon*). PLoS One. 2014;9:e91853.  
400
- 401 14. Iehata S, Nakano M, Tanaka R, Maeda H. Modulation of gut microbiota associated with  
402 abalone *Haliotis gigantea* by dietary administration of host-derived *Pediococcus* sp. Ab1. Fish.  
403 Sci. 2014;80:323–31. doi: 10.1007/s12562-013-0691-9  
404
- 405 15. Iehata S, Inagaki T, Okunishi S, Nakano M, Tanaka R, Maeda H. Improved gut environment  
406 of abalone *Haliotis gigantea* through *Pediococcus* sp. Ab1 treatment. Aquaculture. 2010;305:59–  
407 65. doi: /10.1016/j.aquaculture.2010.04.012  
408
- 409 16. Tanaka R, Ootsubo M, Sawabe T, Ezura Y, Tajima K. Biodiversity and in situ abundance of  
410 gut microflora of abalone (*Haliotis discus hannai*) determined by culture-independent  
411 techniques. Aquaculture. 2004;241:453–63. doi: 10.1016/j.aquaculture.2004.08.032  
412
- 413 17. Huang Z-B, Guo F, Zhao J, Li W-D, Ke C-H. Molecular analysis of the intestinal bacterial  
414 flora in cage-cultured adult small abalone, *Haliotis diversicolor*. Aquac. Res. 2010;41:e760–9.  
415 doi: /10.1111/j.1365-2109.2010.02577.x  
416
- 417 18. Morales-Bojórquez E, Muciño-Díaz MO, Vélez-Barajas JA. Analysis of the Decline of the  
418 Abalone Fishery (*Haliotis fulgens* and *H. corrugata*) along the Westcentral Coast of the Baja  
419 California Peninsula, Mexico. J. Shellfish Res. 2008;27:865–70. doi: 10.2983/0730-  
420 8000(2008)27[865:AOTDOT]2.0.CO;2  
421
- 422 19. SAGARPA. Sustentabilidad y Pesca Responsable en México. Evaluación y Manejo. 2009.  
423
- 424 20. Thompson FL, Gevers D, Thompson CC, Dawyndt P, Hoste B, Munn CB, et al. Phylogeny  
425 and Molecular Identification of Vibrios on the Basis of Multilocus Sequence Analysis. Appl.  
426 Environ. Microbiol. 2005;71:5107–15. doi: 10.1128/AEM.71.9.5107-5115.2005  
427
- 428 21. Hyun DW, Kim MS, Shin NR, Kim JY, Kim PS, Whon TW, et al. *Shimia haliotis* sp. nov., a  
429 bacterium isolated from the gut of an abalone, *Haliotis discus hannai*. Int. J. Syst. Evol.  
430 Microbiol. 2013;63:4248–53. doi: 10.1099/ijs.0.053140-0#tab2  
431
- 432 22. Faust K, Raes J. Microbial interactions: from networks to models. Nat. Rev. Microbiol.  
433 Nature Publishing Group; 2012;10:538–50. doi: 10.1038/nrmicro2832  
434
- 435 23. Chaffron S, Rehrauer H, Pernthaler J, Mering C. A global network of coexisting microbes  
436 from environmental and whole-genome sequence data. Genome Res. 2010;2010:947–59. doi:  
437 10.1101/gr.104521.109  
438
- 439 24. Friedman CS. Infection with *Xenohaliotis californiensis*. Man. Diagnostic Tests Aquat.  
440 Anim. 2012;511–23.  
441  
442

- 443 25. Friedman CS, Andree KB, Beauchamp K a, Moore JD, Robbins TT, Shields JD, et al.  
444 “*Candidatus Xenohaliotis californiensis*”, a newly described pathogen of abalone, *Haliotis* spp.,  
445 along the west coast of North America. *Int. J. Syst. Evol. Microbiol.* 2000;50:847–55. doi:  
446 10.1099/00207713-50-2-847#tab2  
447
- 448 26. Moore JD, Finley C a., Friedman CS, Robbins TT. Withering syndrome and restoration of  
449 southern California abalone populations. *Calif. Coop. Ocean. Fish. Investig. Reports.*  
450 2002;43:112–7.  
451
- 452 27. Crosson LM, Wight N, VanBlaricom GR, Kiryu I, Moore JD, Friedman CS. Abalone  
453 withering syndrome: Distribution, impacts, current diagnostic methods and new findings. *Dis.*  
454 *Aquat. Organ.* 2014;108:261–70. doi: 10.3354/dao02713.  
455
- 456 28. Cáceres-Martínez J, Vásquez-Yeomans R, Flores-Saaib RD. Intracellular prokaryote  
457 *Xenohaliotis californiensis* in abalone *Haliotis* spp. from Baja California, México. *Cienc. Pesq.*  
458 2011;19:5–11. doi: 10.1099/00207713-50-2-847  
459
- 460 29. Balseiro P, Aranguren R, Gestal C, Novoa B, Figueras A. *Candidatus Xenohaliotis*  
461 *californiensis* and *Haplosporidium montforti* associated with mortalities of abalone *Haliotis*  
462 *tuberculata* cultured in Europe. *Aquaculture.* 2006;258:63–72. doi:  
463 10.1016/j.aquaculture.2006.03.046  
464
- 465 30. Horwitz R, Mouton A, Coyne VE. Characterization of an intracellular bacterium infecting  
466 the digestive gland of the South African abalone *Haliotis midae*. *Aquaculture.* 2016;451:24–32.  
467 doi: 10.1016/j.aquaculture.2015.08.024  
468
- 469 31. Brevik OJ, Ottem KF, Kamaishi T, Watanabe K, Nylund A. *Francisella halioticida* sp. nov.,  
470 a pathogen of farmed giant abalone (*Haliotis gigantea*) in Japan. *J. Appl. Microbiol.*  
471 2011;111:1044–56. doi: 10.1111/j.1365-2672.2011.05133.x.  
472
- 473 32. Sjödin A, Svensson K, Ohrman C, Ahlinder J, Lindgren P, Duodu S, et al. Genome  
474 characterisation of the genus *Francisella* reveals insight into similar evolutionary paths in  
475 pathogens of mammals and fish. *BMC Genomics.* 2012;13:268. doi: 10.1186/1471-2164-13-268  
476
- 477 33. Kamaishi T, Miwa S, Goto E, Matsuyama T, Oseko N. Mass mortality of giant abalone  
478 *Haliotis gigantea* caused by a *Francisella* sp. bacterium. *Dis. Aquat. Organ.* 2010;89:145–54.  
479 doi: 10.3354/dao02188  
480
- 481 34. Goecke F, Labes A, Wiese J, Imhoff J. Chemical interactions between marine macroalgae  
482 and bacteria. *Mar. Ecol. Prog. Ser.* 2010;409:267–99. doi: 10.3354/meps08607  
483
- 484 35. Guzman del Prío S a, Serviere-Zaragoza, Siqueiros-Beltrones D. Natural diet of juvenile  
485 abalone *Haliotis fulgens* and *H. corrugata* (Mollusca: Gastropoda) in Bahia Tortugas, Mexico.  
486 *Pacific Sci.* 2003;57:319–24.  
487  
488

- 489 36. Register KB, Thole L, Rosenbush RF, Minion FC. Multilocus sequence typing of  
490 *Mycoplasma bovis* reveals host-specific genotypes in cattle versus bison. *Vet. Microbiol.*  
491 2015;175:92–8. doi: 10.1016/j.vetmic.2014.11.002  
492
- 493 37. Fraser CM, Gocayne JD, White O, Adams MD, Clayton RA, Fleischmann RD, et al. The  
494 Minimal Gene Complement of *Mycoplasma genitalium*. *Science*. 1995;270:397–403. doi:  
495 10.1126/science.270.5235.397.  
496
- 497 38. Heidelberg JF, Eisen J a, Nelson WC, Clayton R a, Gwinn ML, Dodson RJ, et al. DNA  
498 sequence of both chromosomes of the cholera pathogen *Vibrio cholerae*. *Nature*. 2000;406:477–  
499 83. doi: 10.1038/35020000  
500
- 501 39. Colwell RR. Global climate and infectious disease: the cholera paradigm. *Science*.  
502 1996;274:2025–31. doi: 10.1126/science.274.5295.2025  
503
- 504 40. Sawabe T, Inoue S, Fukui Y, Yoshie K, Nishihara Y, Miura H. Mass mortalities of Japanese  
505 abalone *Haliotis discus hannai* caused by *Vibrio harveyi* infection. *Microbes Environ.*  
506 2007;22:300–8. doi: 10.1264/jisme.22.300  
507
- 508 41. Okada K, Iida T, Kita-Tsukamoto K, Honda T. Vibrios commonly possess two  
509 chromosomes. *J. Bacteriol.* 2005;187:752–7. doi: 10.1128/JB.187.2.752-757.2005  
510
- 511 42. Chaiyapechara S, Rungrassamee W, Suriyachay I, Kuncharin Y, Klanhui A, Karoonuthaisiri  
512 N, et al. Bacterial Community Associated with the Intestinal Tract of *P. monodon* in Commercial  
513 Farms. *Microb. Ecol.* 2012;63:938–53. doi: 10.1007/s00248-011-9936-2  
514
- 515 43. Ngangbam AK, Baten A, Waters DLE, Whalan S, Benkendorff K. Characterization of  
516 Bacterial Communities Associated with the Tyrian Purple Producing Gland in a Marine  
517 Gastropod. *PLoS One*. 2015;10:e0140725. doi: 10.1371/journal.pone.0140725  
518
- 519 44. Hassenruck C, Hofmann LC, Bischof K, Ramette A. Seagrass biofilm communities at a  
520 naturally CO<sub>2</sub>-rich vent. *Environ. Microbiol. Rep.* 2015;7:516–25. doi: 10.1111/1758-  
521 2229.12282  
522
- 523 45. Ludwig W, Mittenhuber G, Friedrich CG. Transfer of *Thiosphaera pantotropha* to  
524 *Paracoccus denitrificans*. *Int. J. Syst. Bacteriol.* 1993;43:363–7. doi: 10.1099/00207713-43-2-  
525 363  
526
- 527 46. Ruff-Roberts AL, Kuenen JG, Ward DM. Distribution of cultivated and uncultivated  
528 cyanobacteria and Chloroflexus-like bacteria in hot spring microbial mats. *Appl. Environ.*  
529 *Microbiol.* 1994;60:697–704.  
530
- 531 47. Dowd SE, Callaway TR, Wolcott RD, Sun Y, McKeethan T, Hagevoort RG, et al. Evaluation  
532 of the bacterial diversity in the feces of cattle using 16S rDNA bacterial tag-encoded FLX  
533 amplicon pyrosequencing (bTEFAP). *BMC Microbiol.* 2008;8:125. doi: 10.1186/1471-2180-8-  
534 125

- 535  
536 48. Caporaso JG, Kuczynski J, Stombaugh J, Bittinger K, Bushman FD, Costello EK, et al.  
537 QIIME allows analysis of high-throughput community sequencing data. *Nat. Methods*.  
538 2010;7:335–6. doi: 10.1038/nmeth.f.303  
539  
540 49. Edgar RC. Search and clustering orders of magnitude faster than BLAST. *Bioinformatics*.  
541 2010;26:2460–1. doi: 10.1093/bioinformatics/btq461  
542  
543 50. Caporaso JG, Bittinger K, Bushman FD, Desantis TZ, Andersen GL, Knight R. PyNAST: A  
544 flexible tool for aligning sequences to a template alignment. *Bioinformatics*. 2010;26:266–7. doi:  
545 10.1093/bioinformatics/btp636  
546  
547 51. Haas BJ, Gevers D, Earl AM, Feldgarden M, Ward D V., Giannoukos G, et al. Chimeric 16S  
548 rRNA sequence formation and detection in Sanger and 454-pyrosequenced PCR amplicons.  
549 *Genome Res*. 2011;21:494–504. doi:10.1101/gr.112730.110  
550  
551 52. Hammer Ø, Harper D a. T, Ryan PD. Paleontological statistics software package for  
552 education and data analysis. *Palaeontol. Electron*. 2001;4:9–18.  
553  
554 53. Team RC. A language and environment for statistical computing. R Foundation for Statistical  
555 Computing, Vienna, Austria. URL <http://www.R-project.org/>. [Http://www.R-Project.Org/](http://www.R-Project.Org/). 2015.  
556 p. 2013.  
557  
558 54. Segata N, Izard J, Waldron L, Gevers D, Miropolsky L, Garrett WSW, et al. Metagenomic  
559 biomarker discovery and explanation. *Genome Biol*. [Internet]. 2011;12:R60. doi: 10.1186/gb-  
560 2011-12-6-r60  
561  
562 55. Chao A. Nonparametric Estimation of the Number of Classes in a Population. *Scand J Stat*.  
563 1984;11:265–70. URL: <http://www.jstor.org/stable/4615964>  
564  
565 56. Colwell RK. EstimateS Statistical estimation of species richness and shared species from  
566 samples. Version 9. User’s Guide and application published at <http://purl.oclc.org/estimates.pdf>.  
567 2013.  
568  
569 57. Clarke KR, Warwick RM. A further biodiversity index applicable to species lists: Variation  
570 in taxonomic distinctness. *Mar. Ecol. Prog. Ser*. 2001;216:265–78. doi: 10.3354/meps216265  
571  
572 58. Jaccard P. Nouvelles Recherches Sur la Distribution Florale. *Bull. Soc. Vaudoise Sci. Nat*.  
573 1908;44:223–270.  
574  
575 59. Rahel FJ. Homogenization of Fish Faunas Across the United States. *Science*. 2000;854–6.  
576 doi: 10.1126/science.288.5467.854  
577  
578 60. Kearse M, Moir R, Wilson A, Stones-Havas S, Cheung M, Sturrock S, et al. Geneious Basic:  
579 An integrated and extendable desktop software platform for the organization and analysis of  
580 sequence data. *Bioinformatics*. 2012;28:1647–9. doi: 10.1093/bioinformatics/bts199

581

582 61. Langille M, Zaneveld J, Caporaso JG, McDonald D, Knights D, Reyes J, et al. Predictive  
583 functional profiling of microbial communities using 16S rRNA marker gene sequences. *Nat.*  
584 *Biotechnol.* 2013;31:814–21. doi: 10.1038/nbt.2676

585

586 62. de Voogd NJ, Cleary DFR, Polónia ARM, Gomes NCM. Bacterial community composition  
587 and predicted functional ecology of sponges, sediment and seawater from the thousand islands  
588 reef complex, West Java, Indonesia. *FEMS Microbiol. Ecol.* 2015;91:1–12. doi:  
589 10.1093/femsec/fiv019

590

591 63. Urbanová Z, Bárta J. Microbial community composition and in silico predicted metabolic  
592 potential reflect biogeochemical gradients between distinct peatland types. *FEMS Microbiol.*  
593 *Ecol.* 2014;90:633–46. doi: 10.1111/1574-6941.12422



# Figure 1

## Sampling taxa control

Rarefaction curves of the cumulative number of observed OTUs with increasing number of samples and Chao 1 estimation of total OTU richness in microbiomes of *Haliotis fulgens* (HF) and *H. corrugata* (HC). The vertical line indicates the actual sample size above which the curve is extrapolated to reach Chao 1 estimator.

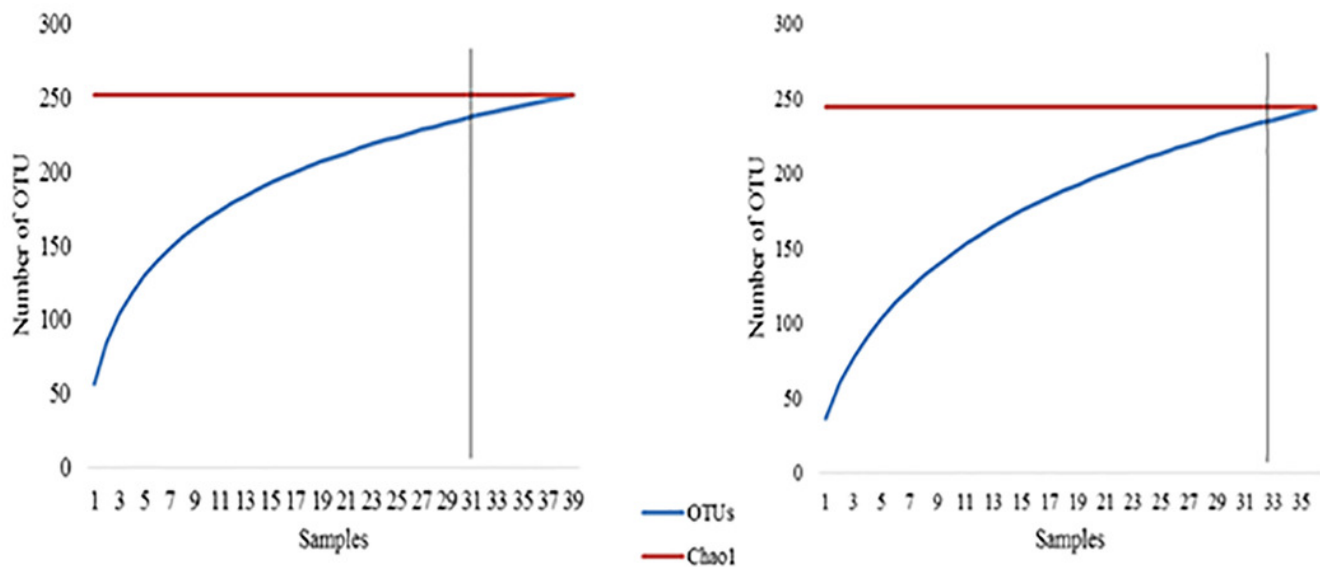


## Figure 2

Abundance of detected bacterial classes

Major bacterial classes comprising the gut microbiota of *Haliotis fulgens* (HF) and *H. corrugata* (HC).

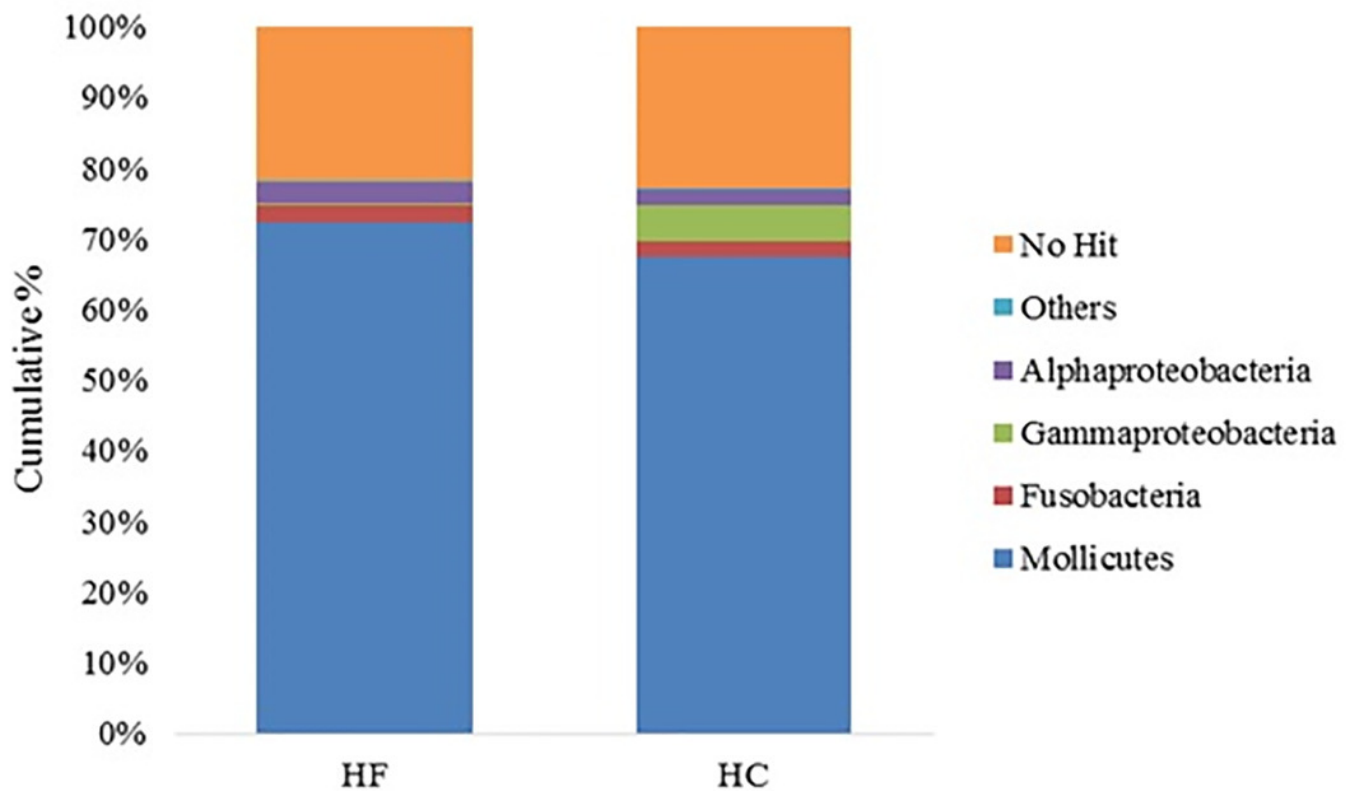


## Figure 3

### Microbiome taxonomic comparison

Non-metric multidimensional scaling (MDS) of Bray Curtis similarity index using  $\log(x+1)$  transformed data based on read abundance of OTUs assembled at 97% similarity cut-off of the gut microbiota of *Haliotis fulgens* (HF) and *H. corrugata* (HC).

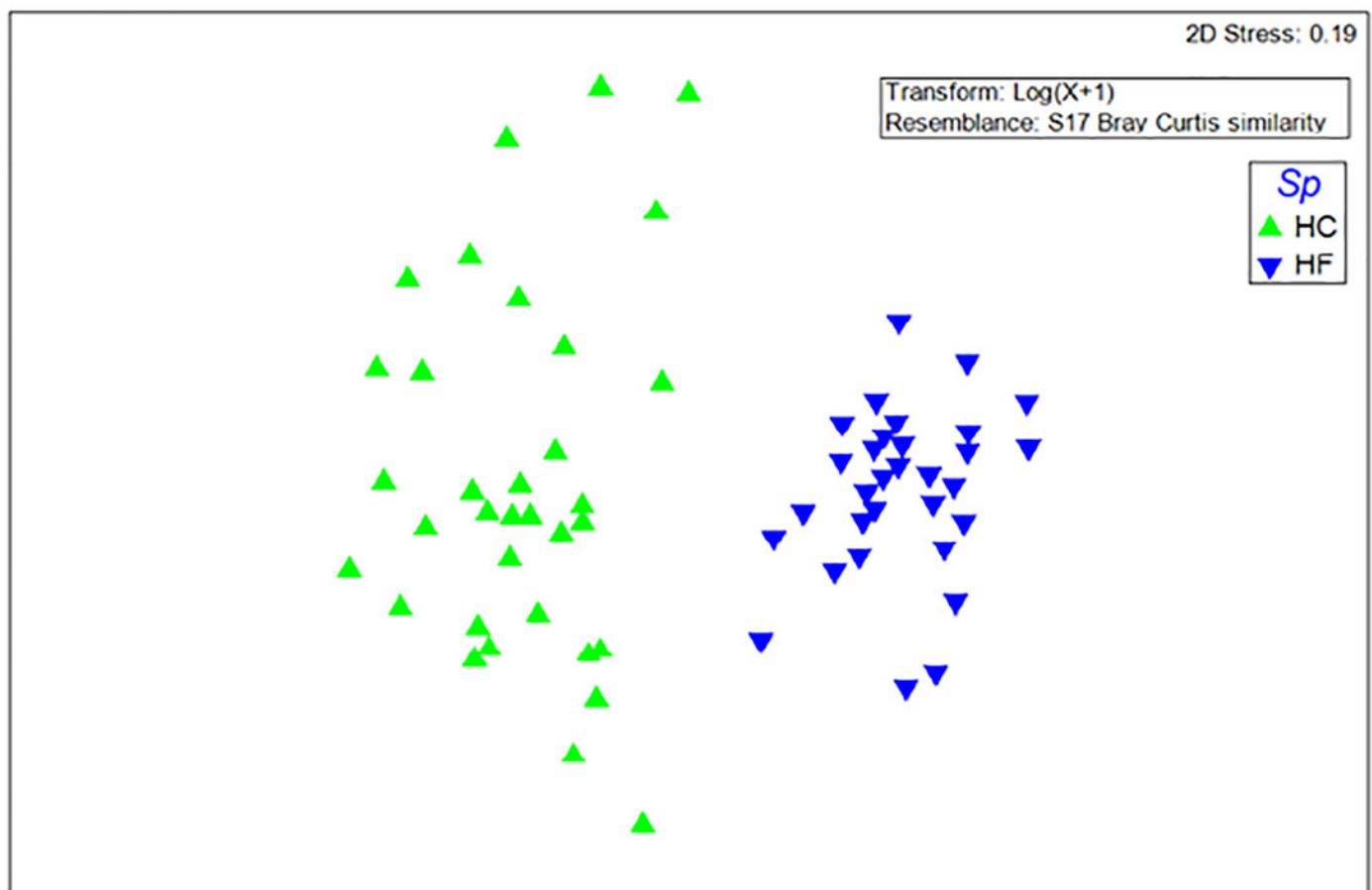


## Figure 4

### Bacterial interactions

Regression analysis of average Jaccard distance based on all pairwise relationships as a function of the number of OTUs (log scale) in microbiomes of *Haliotis fulgens* (HF) and *H. corrugata* (HC).

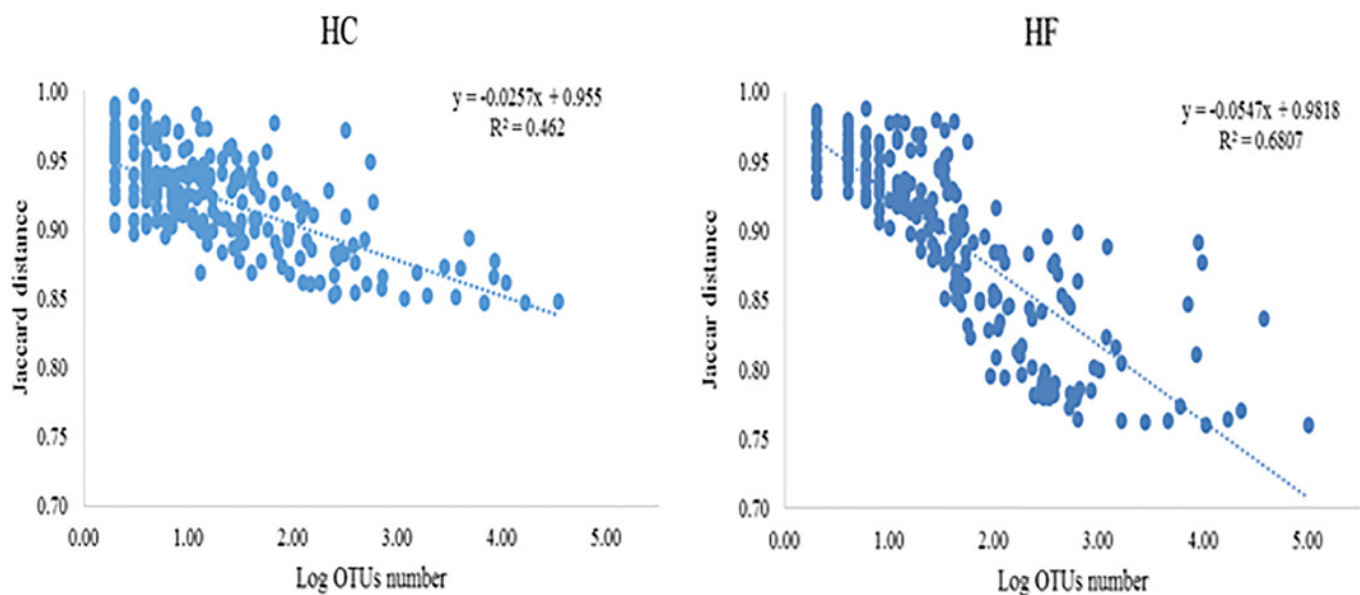


## Figure 5

### Bacterial functional ecology contributions

Bar plots of the relative bacterial gene count contributions of ten KO's within the gut microbiomes of *Haliotis fulgens* (HF) and *H. corrugata* (HC) chosen at random among the 89 most abundant KO's (see text for details).

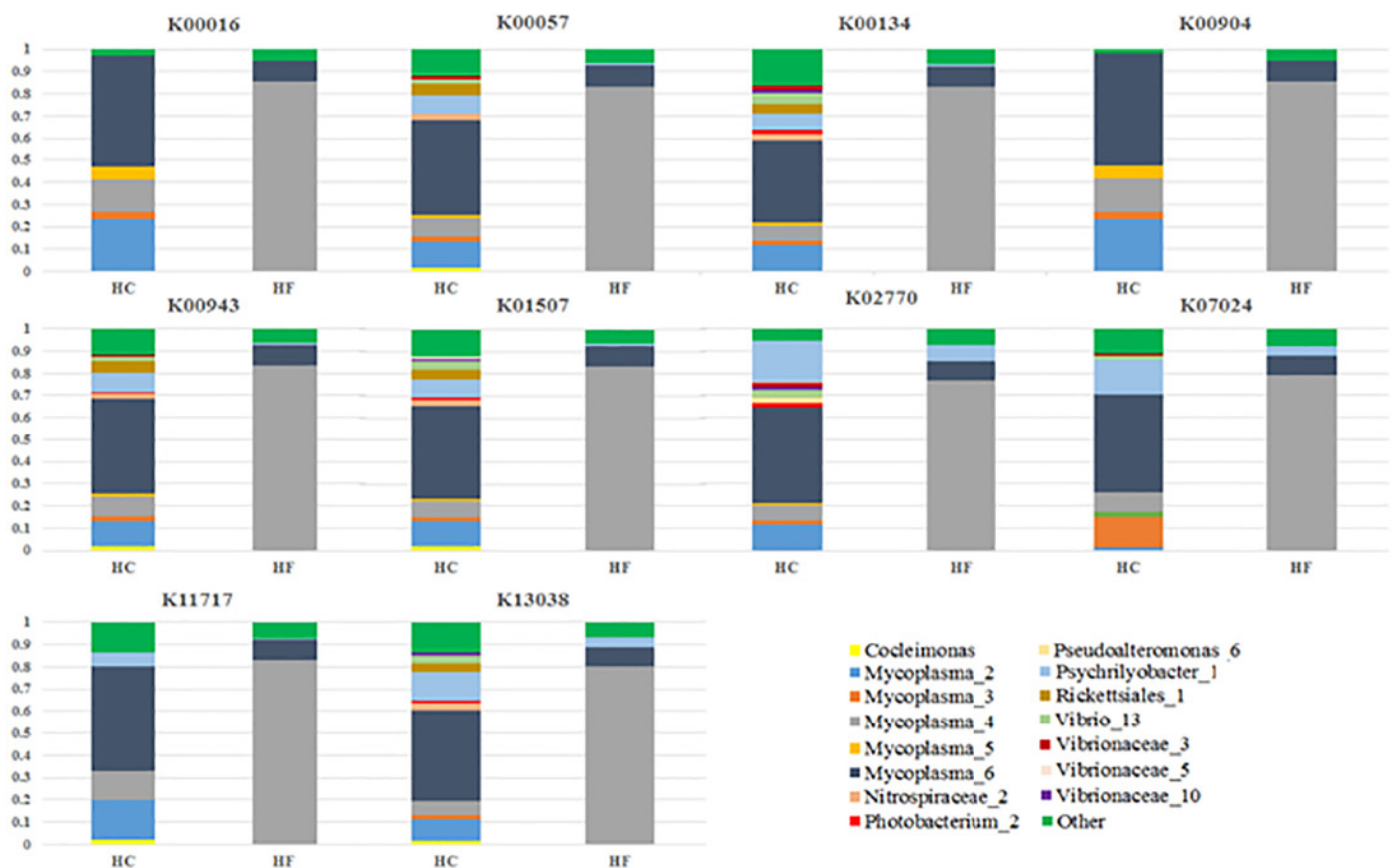


## Figure 6

Comparison of predicted functional ecology

**[A]** Non-metric multidimensional scaling (MDS) of Bray Curtis similarity using  $\log(x+1)$  transformed data of predicted ecological functions in the gut microbiomes of *Haliotis fulgens* (HF) and *H. corrugata* (HC). **[B]** MDS based on Bray Curtis similarity using  $\log(x+1)$  transform data of KEGG orthologue counts in the gut microbiomes of *Haliotis fulgens* (HF) and *H. corrugata* (HC).

